Form Factor of Helical Ribbons

Ian W. Hamley†

Department of Chemistry, University of Reading, Reading, Berkshire RG6 6AD, U.K., and Diamond Light Source, Chilton, Didcot, Oxfordshire OX11 0DE, U.K.

Received July 4, 2008
Revised Manuscript Received October 2, 2008

The misfolding of proteins and peptides can lead to fibrillar aggregates which are often termed amyloid fibrils.[1] These are characterized by a cross-beta structure, with β-strands and polypeptide backbones running perpendicular to the fibril axis, which is coincident with the hydrogen bonding direction. Several types of amyloid fibrils have been shown by high resolution electron microscopy to comprise assemblies of individual twisted β-sheets,[2−5] of which there are two types—tapes or ribbons.[6,7] The two are distinguished by the presence or absence of a hollow core in the fibril. The twist arises from packing constraints of the side groups of the residues within the β-strands.[7]

Helical diffraction theory, as later applied to interpret the structure of DNA,[8] was first applied to calculate the scattering from an α-helical polypeptide, assuming point atoms on a regular helix.[9] The structure factor was also calculated.[9] Expressions for the form factor of helical filaments with negligible cross-section[10] and also with finite cross-section[11] have been provided, and also for pairs of rigid coaxial helical filaments.[10] However, to my knowledge, the form factor of helical ribbons has not previously been reported. Such an expression may be useful when attempting to calculate the diffraction pattern from a twisted β-sheet, in the case that atomic coordinates are not available. The form factor may also be useful in the analysis of small-angle scattering data from other biological systems such as microtubules (for which form factors using atomic coordinates are available[12,13]) or synthetic helical macromolecules such as ladder polymers[14] or peptide amphiphile fibrils.[15]

The form factor of a twisted ribbon of known scattering density only has three parameters, the radius, width and pitch (or equivalently helix angle) (Figure 1). All of these parameters can be estimated from electron microscopy images. However, often TEM cannot provide *in situ* evidence on solution structure, for which a technique such as small-angle scattering is appropriate. For short peptides, the β-sheet width may be a multiple of the β-strand length, which can be estimated from the number of residues incorporated in the strand. In addition to having a small number of input parameters, the form factor presented herein also has a simple analytical form that is readily computed for anisotropic or isotropically averaged configurations.

The form factor of a single helical ribbon of infinitesimal thickness and uniform scattering density ρ can be obtained as follows. The coordinates of a point on the surface are ($R\cos\phi$, $R\sin\phi$, $R\phi\tan\psi + h$).[16] The variables are defined in Figure 1. Here h is a variable along the ribbon axis z, ϕ is the rotation angle around z and ψ is a helical twist angle. The amplitude factor using Cartesian coordinates is then

$$F(\mathbf{q}) = \rho \int \exp[i(q_x R\cos\phi + q_y R\sin\phi + q_z(R\phi\tan\psi + h)]\,\mathrm{d}\mathbf{r} \quad (1)$$

Here $\mathbf{q}$ is the wavevector. The ribbon is a two-dimensional object in three-dimensional space, and the integral can be evaluated using polar coordinates (ϕ, h). Then $\mathrm{d}r = \mathrm{d}\phi\,\mathrm{d}h$. Additionally, using polar coordinates in the same ribbon-fixed axis system for $\mathbf{q} = (q\sin\theta\cos\chi, q\sin\theta\sin\chi, q\cos\theta)$ we obtain

$$F(q,\theta,\chi) = \rho \int\int \exp[i\{qR\sin\theta\cos(\chi-\phi) + q\cos\theta\, R(\phi\tan\psi + h)\}]\,\mathrm{d}\phi\,\mathrm{d}h \quad (2)$$

This integral can be evaluated as follows (here and in the following unimportant numerical prefactors are omitted). Taking first the integral over h, for a single turn of the ribbon, and allowing for centrosymmetry, we obtain

$$\begin{aligned}\int_{R\phi\tan\psi}^{R\phi\tan\psi+\delta} \exp[i(qh\cos\theta)]\,\mathrm{d}h &= \left[\frac{\sin(qh\cos\theta)}{q\cos\theta}\right]_{h=R\phi\tan\psi}^{h=R\phi\tan\psi+\delta} - i\left[\frac{\cos(qh\cos\theta)}{q\cos\theta}\right]_{h=R\phi\tan\psi}^{h=R\phi\tan\psi+\delta} \\ &= \frac{2\cos(b\phi+c)\sin c}{q\cos\theta} + \frac{2i\sin(b\phi+c)\sin c}{q\cos\theta} \\ &= \frac{2\sin c}{q\cos\theta}\exp[i(b\phi+c)] = X(q,\theta,\phi) \quad (3)\end{aligned}$$

Here $b = q\cos\theta R\tan\psi$ and $c = (\delta/2)q\cos\theta$.

The amplitude factor for m repeats of a helical ribbon in a fixed orientation is then given by

$$F(q,\theta,\chi) = \rho\int_0^{m.2\pi} \exp[i(qR\sin\theta\cos(\chi-\phi) + qR\phi\cos\theta\tan\psi)]X(q,\theta,\phi)\,\mathrm{d}\phi \quad (4)$$

This is the amplitude factor of a single helical ribbon in a fixed orientation (ϕ, ψ, θ). The integral over ϕ may not be determined analytically in a straightforward manner, however this equation is readily evaluated numerically. The form factor may be calculated as $I(q,\theta,\chi) = F(q,\theta,\chi)F^*(q,\theta,\chi)$ using eq 4. The experimentally measured intensity in dilute solution will be related to $I(q,\theta,\chi)$ by a multiplicative constant, depending on incident intensity, polarization *etc*.

Figure 2 presents examples of the anisotropic form factor from aligned helical ribbons. The circular symmetry in the (q_x, q_y) plane reflects the projected symmetry along the axis of the helical ribbon. The scattering in the (q_x, q_z) and (q_y, q_z) planes is found to be dominated by intensity in layer lines at $q_z = n\pi/p$, the intensity being more concentrated as m, i.e., the number of helical repeats, increases. This can be understood as follows. The integral in eq 4 can be evaluated using the fact that[9]

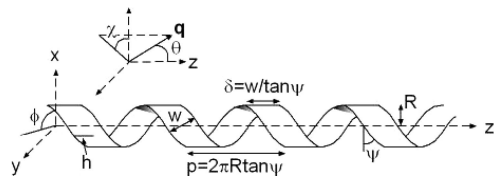

Figure 1. Bottom: Single infinitesimally thick helical ribbon showing definition of variables.[16] Top: Scattering vector $\mathbf{q}$ and associated polar angles in the ribbon-fixed reference frame.

† E-mail: I.W.Hamley@reading.ac.uk.

10.1021/ma8014917 CCC: $40.75
Published on Web 10/29/2008

$$\int_0^{2\pi} \exp[ia\cos(\chi-\phi)+in\phi]\,d\phi = 2\pi i^n J_n(a)\exp(in\chi) \quad (5)$$

Here $a = qR\sin\theta$. Using this relationship we obtain, for $q\cos\theta = q_z = n\pi/p$

$$F_n(q,\theta,\chi) = \rho 2\pi i^n J_n(qR\sin\theta)\frac{2\sin c}{q\cos\theta}\exp(ic)\exp(in\chi) \quad (6)$$

This is the form factor derived for a helix[9] convoluted with the term $2\sin c\exp(ic)/[q\cos\theta]$ contained in $X(q,\theta,\phi)$ which results from the width of the ribbon.

The oscillations in the amplitude factor in Figure 2 result from the Bessel functions in Eq. 6, those on the $n = 0$ layer line are maximal at $q_\perp = 0$ (here $q_\perp$ is q_x or q_y) as is the zeroth order Bessel function, those for $n \neq 0$ have a minimum at $q_\perp = 0$ as do the $J_n(z)$ values with $n = 1, 2,....$

In practice, it would be very difficult to measure the form factor of aligned helical ribbons in a sufficiently dilute solution (although a suitable contrast variation experiment in neutron scattering might help). Therefore it is of more interest to examine the isotropically averaged form factor. Assuming that the intensity is totally concentrated on the layer lines, we take the isotropic average as the sum of the isotropically averaged intensities on the layer lines:

$$I(q) = \rho^2 \sum_{n=-\infty}^{\infty}\int_0^{\pi/2} F_n F_n^* \sin\beta\,d\beta$$

$$= \rho^2 \sum_{n=-\infty}^{\infty} i^{2n}\int_0^{\pi/2} \frac{\sin^2\left(\frac{\delta}{2}q'_z\right)}{q'^2_z} J_n^2(q'_\perp R\sin\beta)\sin\beta\,d\beta \quad (7)$$

Here $q_\perp = \sqrt{(q^2 - n^2\pi^2/p^2)}$, $q'_\perp = q_\perp\cos\beta - q_z\sin\beta$ and $q'_z = q_\perp\sin\beta + q_z\cos\beta$. The latter terms result from the averaging around the angle β defined in Figure 2c.

In practice, the sum in Eq. 7 only has to extend over the layer lines in the q range accessed, which can readily be determined from the position of the nth layer line at $q_z = n\pi/p$. Figure 3 contains SAXS intensity profiles calculated using the approximate formula, Eq. 7, along with calculated form factor profiles for a hollow tube (*vide infra*). Figure 3 shows the form factor calculated with terms up to $n = 2$. In fact the sum is convergent, and indeed the total intensity is generally dominated by the $n = 0$ contribution. The periodicity of the oscillations in the form factor depends mainly on R, but is modulated by w and p. The scaling behavior at large q is approximately $I(q) \sim q^{-2}$, depending somewhat on w and p. This scaling behavior can be rationalized on the basis of the following analysis.

Equations 4−7 are valid for $p \equiv 2\pi b > 2\delta$. In the limiting case $p = 2\delta$, we have an infinitesimal cylindrical tube (length P) for which $X(q, \theta, \phi) = 1$ and the isotropically averaged form factor is given exactly by

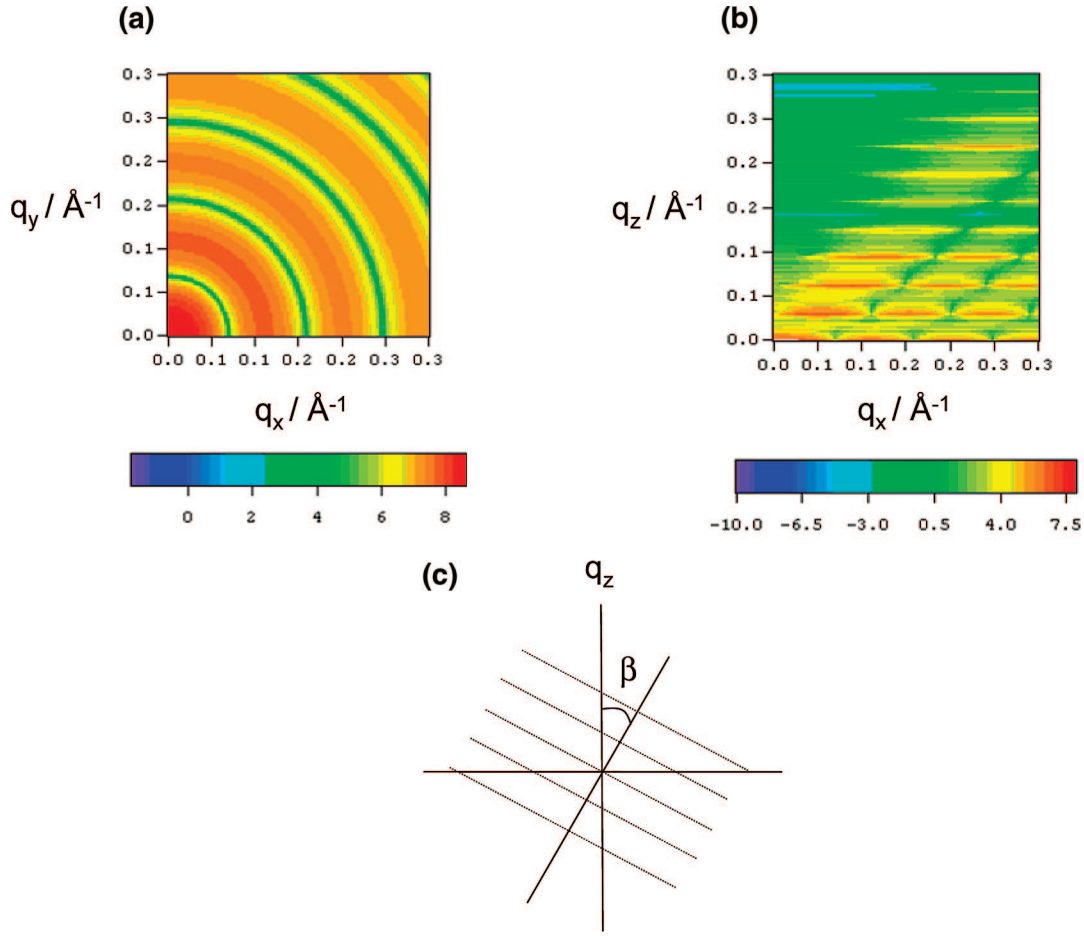

Figure 2. Examples of anisotropic form factors obtained for an aligned ribbon with $R = 35$ Å, $w = 20$ Å, $p = 100$ Å and $m = 20$ repeats. (a) q_x, q_y plane (q_y vertical, scale in Å^{-1}), (b) q_x, q_z plane (q_z vertical, scale in Å^{-1}). The intensity scales are logarithmic. One quadrant of the scattering pattern is shown in each case. (c) Definition of angle β used in isotropic averaging of layer line intensities.

$$I(q) = \rho^2 \int_0^{\pi} \left(\frac{\sin\left(\frac{1}{2} qp \cos\theta\right)}{\frac{1}{2} qp \cos\theta} \right)^2 J_0^2(qR \sin\theta) \sin\theta \, d\theta \quad (8)$$

This is analogous to the dominant $n = 0$ term in eq 7, although in the case of ribbons the form factor also depends on the ribbon width, via δ.

In order to understand the scaling behavior with q more clearly, one may take the limit of the scattered intensity from an infinite cylinder in the case $p \to \infty$. Following Porod,[17] the scattering from the cross-section (R dependence) can be separated from the axial factor (p dependence) The resulting scaling is $I(q) \sim q^{-2}$ for an infinite flat sheet or $I(q) \sim q^{-1}$ for a rod with infinitesimal cross-section.[17] The total intensity in eq 8 for an infinite tube (which is a wrapped sheet) scales as q^{-2} at large q. This behavior is confirmed numerically for finite but large p (Figure 3). For the helical ribbon, a similar scaling behavior is observed for large p, modulated slightly by w or p. Comparison of the form factors for ribbons and tubes, indicates that the first minimum for the ribbons is in a different position to that for tubes with the same value of R, and depends on w and p. This may be useful in distinguishing ribbons from tapes, even in the case of significant polydispersity which will reduce the amplitude of form factor oscillations. Indeed the amplitude of the form factor oscillations is greatly reduced for ribbons, depending strongly on w and p (in contrast to the case of tubes). Form factor calculations are also useful beyond calculations of dilute solution scattering, entering into expressions for the structure factor for instance in random phase approximation calculations.[18] Equation 7 can be generalized to allow for polydispersity in radius by a further integral over an appropriate radius distribution function in the usual way.[19]

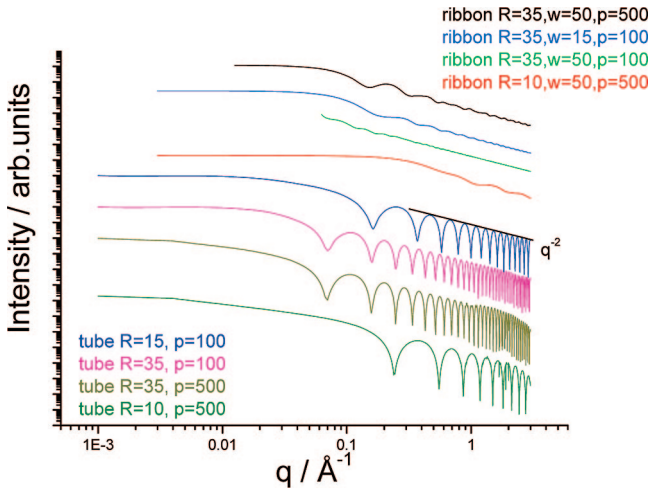

Figure 3. Isotropically averaged form factors for helical ribbons (top, Eq. 7 with terms up to $n = 2$) and hollow tubes (bottom). Particle dimensions (in Å) are indicated.

In summary, expressions are provided for the form factor of helical ribbons. An exact expression is provided for the form factor an oriented ribbon. For a large number of helical repeats, the intensity is concentrated on layer lines. This facilitates the calculation of an approximate expression for the form factor for an isotropically averaged ensemble of ribbons. The form factor oscillation period is controlled mainly by the fibril radius. The intensity at high q scales approximately as q^{-2} depending on pitch p and width w, this being similar to the scaling observed for infinitesimal hollow tubules. The form factors provided are expected to be useful in the analysis of small-angle scattering from various types of twisted macromolecules, especially beta-sheet amyloid fibrils.

Acknowledgment. I thank Dr Valeria Castelletto, Prof Alexei Likhtman (Reading) and Prof Jan Skov Pedersen (Aarhus) for helpful comments.

References and Notes

(1) Hamley, I. W. *Angew. Chem., Int. Ed. Engl.* **2007**, *46*, 8128–8147.
(2) Sunde, M.; Blake, C. C. F. *Q. Rev. Biophys.* **1998**, *31*, 1–39.
(3) Serpell, L. C.; Blake, C. C. F.; Fraser, P. E. *Biochemistry* **2000**, *39*, 13269–13275.
(4) Jimenez, J. L.; Nettleton, E. J.; Bouchard, M.; Robinson, C. V.; Dobson, C. M.; Saibil, H. R. *Proc. Natl. Acad. Sci. U.S.A.* **2002**, *99*, 9196–9201.
(5) Rubin, N.; Perugia, E.; Goldschmidt, M.; Fridkin, M.; Addadi, L. *J. Am. Chem. Soc.* **2008**, *130*, 4602–4603.
(6) Aggeli, A.; Nyrkova, I. A.; Bell, M.; Harding, R.; Carrick, L.; McLeish, T. C. B.; Semenov, A. N.; Boden, N. *Proc. Natl. Acad. Sci. U.S.A.* **2001**, *98*, 11857–11862.
(7) Fishwick, C. W. G.; Beevers, A. J.; Carrick, L. M.; Whitehouse, C. D.; Aggeli, A.; Boden, N. *Nano Letters* **2003**, *3*, 1475–1479.
(8) Wilkins, M. H. F.; Stokes, A. R.; Wilson, H. R. *Nature (London)* **1953**, *171*, 738–740.
(9) Cochran, W.; Crick, F. H. C.; Vand, V. *Acta Crystallogr.* **1952**, *5*, 581–586.
(10) Schmidt, P. W. *J. Appl. Crystallogr.* **1970**, *3*, 257–264.
(11) Pringle, O. A.; Schmidt, P. W. *J. Appl. Crystallogr.* **1971**, *4*, 290–293.
(12) Metoz, F.; Wade, R. H. *J. Struct. Biol.* **1997**, *118*, 128–139.
(13) Knupp, C.; Squire, J. M. *J. Appl. Crystallogr.* **2004**, *37*, 832–835.
(14) Hickl, P.; Ballauff, M.; Scherf, U.; Müllen, K.; Lindner, P. *Macromolecules* **1997**, *30*, 273–279.
(15) Fukuda, H.; Goto, A.; Imae, T. *Langmuir* **2002**, *18*, 7107–7114.
(16) Chung, D. S.; Benedek, G. B.; Konikoff, F. M.; Donovan, J. M. *Proc. Natl. Acad. Sci. U.S.A.* **1993**, *90*, 11341–11345.
(17) Porod, G. In *Small-Angle X-ray Scattering*; Glatter, O., Kratky, O., Eds.; Academic Press: London, 1982.
(18) de Gennes, P. G. *Scaling Concepts in Polymer Physics;* Cornell University Press: Ithaca, NY, 1979.
(19) Pedersen, J. S. *Adv. Colloid Interface Sci.* **1997**, *70*, 171–210.

MA8014917